4. Examples

To illustrate the use of the concepts, consider the specific case of a Lorentz oscillator medium where $\chi(\omega)$ has the form

$$\chi(\omega) = \sum_{j=1}^{N} \chi_j(\omega) = \sum_{j=1}^{N} \frac{f_j \omega_{p_j}^2}{\omega_j^2 - i\gamma_j \omega - \omega^2}. \tag{42}$$

The parameters f_j, ω_{p_j}, ω_j, and γ_j are the oscillator strength, plasma frequency, resonant frequency, and damping rate of the j^{th} Lorentz oscillator. We consider a Gaussian pulse of the form

$$E_i(t) = E_0 e^{-t^2/\tau^2} \cos(\bar{\omega} t + \phi) \tag{43}$$

incident on this medium and study the energy dynamics in this interaction.

For our first example, consider a double resonance medium with parameters

$$\begin{aligned} \gamma_1 &= 0.1\gamma_2 \\ \omega_1 &= \omega_2 = 100\gamma_2 \\ f_1\omega_{p_1}^2 &= -9.95\gamma_2^2 \\ f_2\omega_{p_2} &= 100\gamma_2^2 \\ L &= c/\gamma_2 \end{aligned} \tag{44}$$

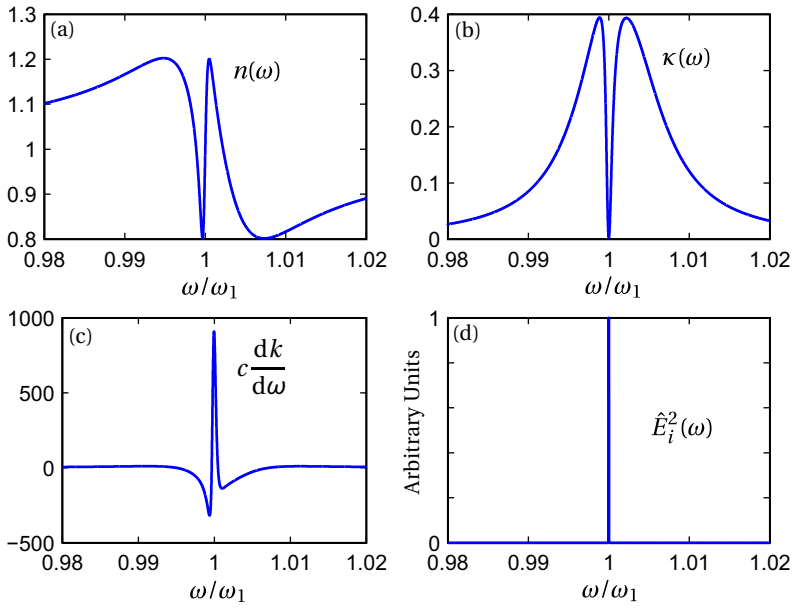

Fig. 1. The real (a) and imaginary (b) parts of the the index of refraction for the parameters in Eq. (44). (c) The group delay function for this medium. (d) The power spectrum of the pulse, which has been arbitrarily normalized to have a maximum value of one. This pulse-medium combination should exhibit moderately slow propagation delays, around 900 times slower than c.

For our incident field, we choose a relatively narrowband pulse with

$$\begin{aligned} \tau &= 1000\gamma_2^{-1} \\ \bar{\omega} &= 100\gamma_2 \\ \phi &= 0. \end{aligned} \tag{45}$$

Figures 1(a)–1(c) plot $n(\omega)$, $\kappa(\omega)$, and $\mathrm{d}k/\mathrm{d}\omega$ (the group delay function) for this medium. Note that the pulse spectrum is centered in a mostly transparent region where index varies rapidly, resulting in a group delay function that predicts moderately slow delay times about 900 times slower than c. We calculated the spatial distribution of the energy densities associated with this pulse, and Fig. 2 shows an animation of the evolution of the distribution as time progresses. Figure 2(a) shows the large scale behavior of this pulse as it moves from the vacuum on the left, through the medium (indicated by the vertical green line), and then into the vacuum on the right. The blue solid line indicates the distribution of field energy, while a dotted red line indicates how the pulse would have propagated if the medium were not there for comparison. In both cases we have time-averaged the rapid fluctuations at the optical frequency to give on the smooth envelope of the distributions. As expected, the pulse propagates slowly through t medium and emerges during the trailing edge of the dotted reference pulse.

Figure 2(b) plots $u_{\mathrm{field}}(z,t)$ and Fig. 2(c) plots $u_{\mathrm{int}}(z,t)$ in the medium. The field energy the medium is the portion of the energy that is actively being transported, and shows a pe traversing the medium approximately 900 times slower than c. The total energy in the mediu

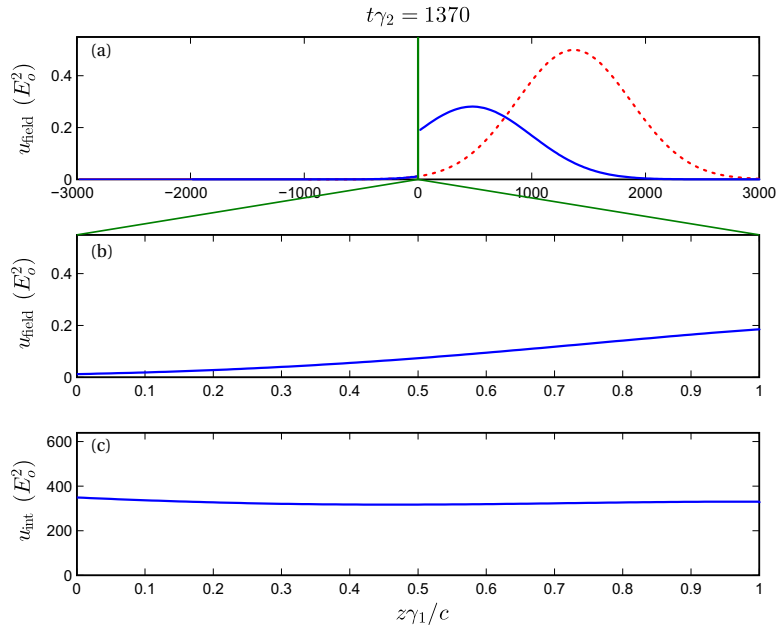

Fig. 2. An animation of the spatial distribution of energy densities as the pulse defined in Eq. (45) traverses the medium defined in Eq. (44) (Media 1). (a) The propagation in vacuum before and after the medium, represented by the vertical line at $z = 0$. The solid line plots the field energy distribution with the medium present and the dotted line plots the field energy distribution would have been if the medium were not present for comparison. (b) The distribution of u_{field} in the medium. (c) The distribution of u_{int} in the medium. All plots have been locally time-averaged to remove the rapid fluctuations at the carrier frequency.

#203993 - $15.00 USD Received 3 Jan 2014; revised 11 Feb 2014; accepted 12 Feb 2014; published 19 Feb 2014

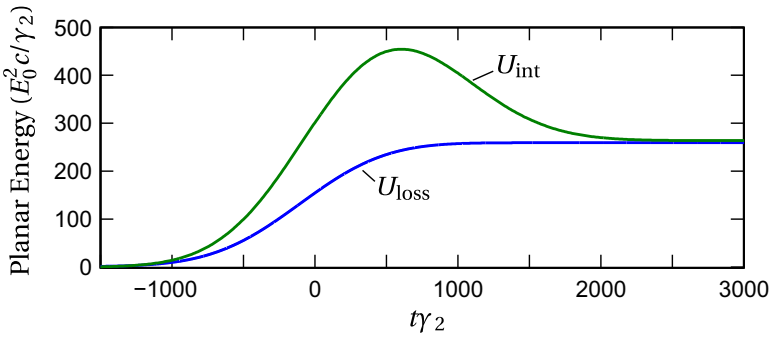

Fig. 3. The total energy stored in the medium $U_{\rm int}$ compared with the real-time loss $U_{\rm loss}$ of energy for the pulse-medium combination illustrated in Fig. 2.

$U_{\rm int}(t)$ is stationary, and can be divided into a portion $U_{\rm trans}$ that could be transmitted with the appropriate future pulse, and a portion $U_{\rm loss}$ that must remain in the medium.

Figure 3 plots the total energy stored in the medium $U_{\rm int}(t)$ compared with the real-time loss $U_{\rm loss}(t)$ calculated using Eq. (40). $U_{\rm trans}$ is the difference of these two curves. Comparing $U_{\rm field}$ to $U_{\rm trans}$, we find that only about 0.2% of the undissipated energy is actually moving via Poynting flux at any given time while the rest remains stationary in the medium. Thus, the average speed of all the energy is heavily influenced by the stationary portion of the energy and the dramatic slow propagation is observed.

Notice that a large fraction of the incident energy is lost from this Gaussian pulse during the times when it is entering the medium. Eventually, the remaining energy is transmitted into the vacuum to the right, and $U_{\rm int}$ and $U_{\rm loss}$ take on the same value at large times (i.e. all the energy remaining in the medium has been dissipated). We can engineer a more efficient extraction of energy by using Eq. (37) to calculate a second half of a pulse that will extract all energy available in the medium after a certain time. We take the pulse before $t = 0$ to be as defined by Eq. (45), and after $t = 0$ we append the optimal recovery pulse calculated by Eq. (37). Figure 4(a) shows the temporal profile of the original incident pulse, and Fig. 4(b) shows the pulse with the optimum recovery field appended to the second half.

Figure 5 shows an animation of the pulse in Fig. 4(b) propagating through the medium defined by Eq. (44). The optimum field contains a delta function represented by the arrow in Fig. 4(b). This feature is not resolved in the animation because it is much too narrow for the

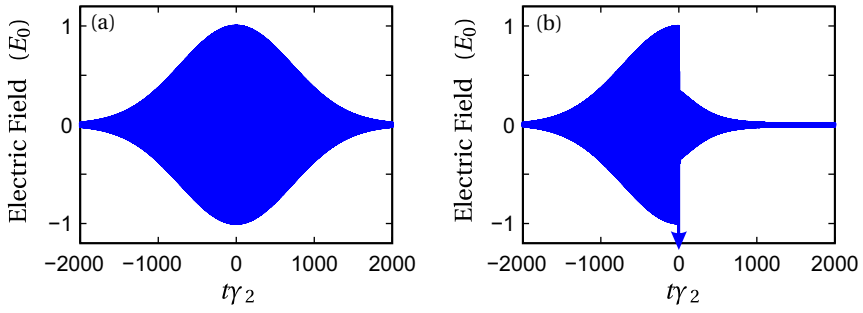

Fig. 4. (a) The temporal profile of a the Gaussian pulse Eq. (43) with the parameters in Eq. (45). (b) The first half of the pulse is the same as (a), but the second half is the optimum future recovery field for the medium described in Eq. (44).

#203993 - $15.00 USD Received 3 Jan 2014; revised 11 Feb 2014; accepted 12 Feb 2014; published 19 Feb 2014

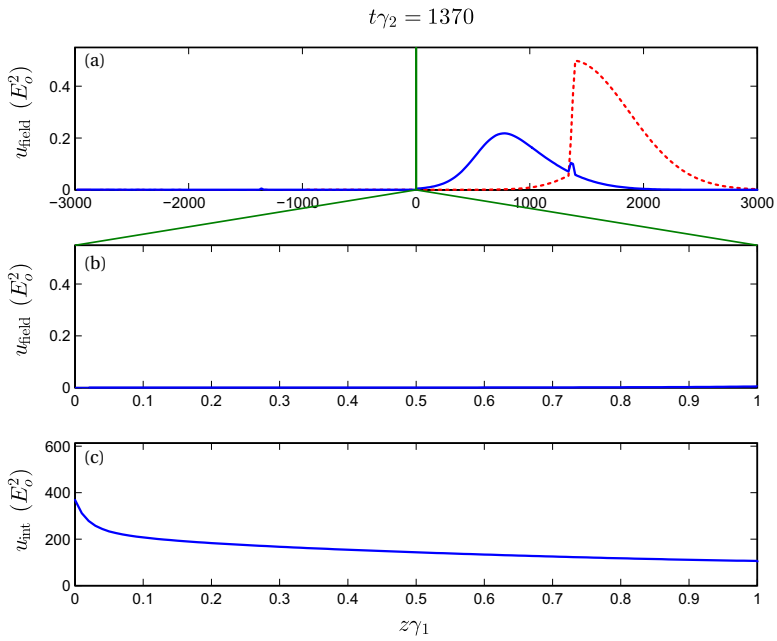

Fig. 5. An animation of the spatial distribution of energy densities as the pulse defined in Eq. (45) traverses the medium defined in Eq. (44) (Media 2). (a) The propagation in vacuum before and after the medium, represented by the vertical line at $z = 0$. The solid line plots the field energy distribution with the medium present and the dotted line plots the field energy distribution would have been if the medium were not present for comparison. (b) The distribution of u_{field} in the medium. (c) The distribution of u_{int} in the medium. All plots have been locally time-averaged to remove the rapid fluctuations at the carrier frequency.

resolution of the movie, but is included in the calculations used to generate the movie. A true delta function would not be possible to create in a physical experiment. Nevertheless, in our simulation a narrow downward peak in the pulse profile is sufficient to capture the essential behavior of the recovery field.

For the example parameters we have chosen, there is very little reflected light because the index of refraction for the medium is near unity for the frequencies in the pulse. In cases where there is significant reflection, the recovery field can contains repeated pulses separated by the round-trip traversal time of the medium. This sequence of pulses results from our requirement that the optimal recovery pulse cause the maximum amount of light to be transmitted, rather than just removed from the medium. The sequence of afterpulses interferes with the backward traveling portion of the field in the medium so as to cause the energy to be transmitted to the right rather than reflected to the left. If one wishes to avoid this feature in a recovery pulse, it is necessary use Eq. (41) in calculating the recovery field as discussed previously.

In Fig. 6 we plot the real-time loss U_{loss} and the total energy in the medium U_{int} for this modified pulse. For comparison, the plots from Fig. 3 (for the unmodified pulse in Fig. 4(a)) are repeated as dashed lines. Note that after $t = 0$, when we switch to the optimal recovery field, there is no additional loss for this pulse. The energy that has been deposited in the medium prior to $t = 0$ is extracted by the optimum recovery field and produces the delayed portion of energy transmitted to the vacuum after the medium.

#203993 - $15.00 USD Received 3 Jan 2014; revised 11 Feb 2014; accepted 12 Feb 2014; published 19 Feb 2014

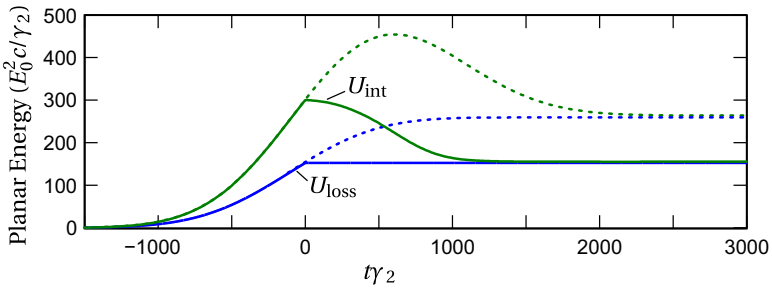

Fig. 6. The solid lines plot the total energy stored in the medium $U_{\rm int}$ and the real-time loss $U_{\rm loss}$ of energy for the pulse-medium combination illustrated in Fig. 5. Dashed lines plot the same quantities from Fig. 3 for comparison.

5. Conclusion

We have introduced a method for calculating the real-time loss of energy stored in a medium that is valid for pulses propagating in extended media. This method for calculating dissipation is consistent with Maxwell's equations and allows one to analyze real-time loss in propagation settings. A complete understanding of real-time loss is important in applications such as slow and fast pulse propagation experiments where the timing of energy flows in and out of the pulse are crucial. We have illustrated the use of this formalism in analyzing a typical "slow light" propagation situation, and illustrated a simple method for engineering pulse shapes for optimal energy recovery. While this example employed a specific model (the Lorentz model), the formalism is independent of the model used to represent the material.

#203993 - $15.00 USD Received 3 Jan 2014; revised 11 Feb 2014; accepted 12 Feb 2014; published 19 Feb 2014